Nanostructured silicon formations as a result of ionized N2 gas reactions on silicon with native oxide layers

Min-Cherl Jung, Tae Gyoung Lee, Young Ju Park, Sung Ho Jun, Joosang Lee et al.

Citation: Appl. Phys. Lett. **82**, 3653 (2003); doi: 10.1063/1.1579124
View online: http://dx.doi.org/10.1063/1.1579124
View Table of Contents: http://apl.aip.org/resource/1/APPLAB/v82/i21
Published by the American Institute of Physics.

Nanostructured silicon formations as a result of ionized N_2 gas reactions on silicon with native oxide layers

Min-Cherl Jung,[a] Tae Gyoung Lee, and Young Ju Park[b]
Nano-device Research Center, Korea Institute of Science and Technology, 136-791, Korea

Sung Ho Jun, Joosang Lee, and Moonsup Han
Department of Physics, University of Seoul, Seoul 130-743, Korea

Jong Seok Jeong and Jeong Yong Lee
Department of Material Science and Engineering, Korea Advanced Institute of Science and Technology, 305-701, Korea

(Received 18 November 2002; accepted 31 March 2003)

Nanostructured silicon was formed by means of the ionized N_2 gas reaction on SiO_2/Si, and the electronic structure, surface morphology, and optical properties were investigated. The physicochemically modified thin layers were resolved to SiN_y and SiO_xN_y through the observation of Si $2p$, O $1s$, and N $1s$ core-level spectra in x-ray photoelectron spectroscopy. The formations of SiO_xN_y and SiO_2 nanostructures (3–4 nm in size), performed by the etching process followed by adsorption of ionized nitrogen, were confirmed by atomic force microscopy. The nanocrystalline Si (6 nm in size) distributed within the modified layer (approximately 10 nm thick) was observed after the *in situ* rapid thermal annealing processes, using high-resolution transmission electron microscopy. Photoluminescence with a wavelength peaking at around 400 nm was emitted from the nanocrystalline Si formed from the $SiO_xN_y/SiO_2/Si$ structures. This work suggests that the nanocrystalline-Si formation and the nanostructured surface modification method, using the controlled ionized gas, were simple and efficient methods requiring low energy and low temperatures. © *2003 American Institute of Physics.* [DOI: 10.1063/1.1579124]

Recently, many researchers have reported on the potential applications of Si-based devices in optoelectronics.[1–3] Since the visible photoluminescence (PL) in porous Si (p-Si) was reported at room temperature (RT), many scientists have endeavored to understand the structure, electronic properties, luminescence mechanisms, etc.[4–6] P-Si can be produced by anodic oxidation of a crystalline silicon anode, typically for visible light emissions. However, the mechanism of light emission from p-Si is not fully understood. Various nanostructures, such as amorphous silicon (a-Si) and nanocrystalline silicon (nc-Si), were also reported for the light-emitting device applications.[7,8] Plasma-enhanced chemical vapor deposition was utilized mostly in the production of a-Si and nc-Si.[9] A typical formation mechanism for the nanostructured Si (ns-Si) is based on a self-organized mechanism: The transformation from nonstoichiometric thin layers of SiN_x or SiO_x/Si into ns-Si embedded in a stoichiometric Si_3N_4 or SiO_2 through the postgrowth thermal annealing processes.[10] However, the primary flaw in such a formation mechanism is that the size and distribution of ns-Si are difficult to control. Hydrogen atoms that are introduced by ion implantation, plasma, and thermal dissociation of H_2 or NH_3, etc., can be good candidates for a nanometric control medium.[11,12]

In this article, a feasible method for the formation of ns-Si using ionized N_2 gas reactions on SiO_2/Si at RT is reported. Since the ionized gas reaction method is a type of low-energy plasma exposure with no emission of photons, it has many advantages, e.g. easy control, low surface damage, low-temperature process, etc.

The silicon substrates used in this work had Sb-doped (001) orientation with a resistivity of 0.01 Ω cm and were commercial products of Nilaco Corporation. The native oxide layer on Si was cleaned using the Radio Corporation of America process in an air atmosphere. Samples were put into the ultrahigh-vacuum (UHV) chamber (background pressure 1×10^{-10} torr). The vacuum system was composed of an analysis chamber for the x-ray photoelectron spectroscopy (XPS) experiment, and an ion beam treatment chamber for the surface modifications. Samples were exposed to the ionized N_2 gas (N_2 99.999%) using an AG5000 cold cathode ion gun of the VG microtech at room temperature. The sample holder was voltage biased to -1 kV. The exposing gas pressure was typically maintained at 4.0×10^{-6} torr. The exposure time varied from 5 to 180 min. The typical sample current density was approximately 0.15 $\mu A/cm^2$. Typical fabrication yields are high because the process conditions are reliable. Physicochemically modified silicon surfaces were investigated by XPS and atomic force microscopy (AFM). The Si $2p$, O $1s$, and N $1s$ core-level spectra and the binding energy 99.3 eV of Si $2p_{3/2}$ for the clean silicon were obtained by referencing core-level Au $4f_{7/2}$. The structural analysis was performed, and the luminescent properties of the ns-Si were determined using high-resolution transmission electron microscopy (HR-TEM) and PL measurement, respectively.

Figures 1(a)–1(c) show Si $2p$, O $1s$, and N $1s$ core-

[a]Also at: Department of Physics, University of Seoul, Seoul 130-743, Korea.
[b]Author to whom correspondence should be addressed; electronic mail: yjpark@kist.re.kr

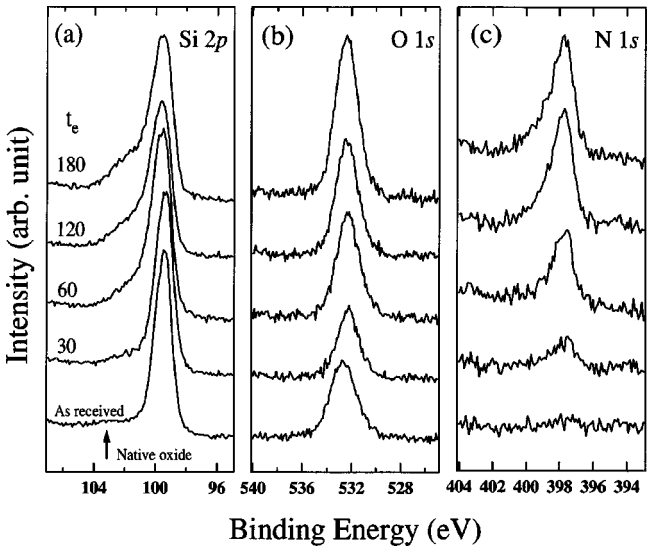

FIG. 1. (a) Si $2p$, (b) O $1s$, and (c) N $1s$ core-level spectra with various ionized N_2 gas exposure times. The working pressure was 4×10^{-6} torr and the sample was voltage biased to -1 kV at RT.

level spectra for the samples, with ionized N_2 gas exposure times (t_e) of 30, 60, 120, and 180 min. The peak position of native silicon oxide is marked by an arrow at 102.9 eV, which is at a higher binding energy than the main bulk-Si peak observed at 99.3 eV, as shown in Fig. 1(a). The spectral weight in between the arrow mark and the main peak position increases with increasing t_e. In Fig. 1(b), it is apparent that the binding energy of O $1s$ is 533.0 eV for an as-received sample, and it shifts toward a lower value with increasing t_e. It should also be noted that the N $1s$ core-level spectrum was not apparent before ionized N_2 gas exposure. However, the peak intensity of the N $1s$ core-level was enhanced with increasing t_e. The peak position of the O $1s$ core-level was consistently shifted to a low binding energy and the peak intensity became conspicuous as the t_e increased. The shifts of peak positions were due to the creation of intermediate states such as SiO_xN_y and SiN_y between SiO_2 and Si.[13] This means that the N $1s$ core-level spectra have several phases of chemical composition, resulting from the ionized N_2 gas exposure onto the SiO_2/Si surfaces. In addition, the spectral intensity of the Si $2p$ core level, denoted by an arrow mark [Fig. 1(a)], increased with t_e, also indicating the chemical modification of SiO_2/Si surfaces.

Figures 2(a)–2(d) show the AFM surface morphology of the ionized N_2 gas-exposed surface at various t_e. For the sample at $t_e\leqslant30$ min, it was found from the AFM data analysis that nanostructures with an average height of 3.7 nm were distributed over the surface. This means that the native SiO_2 thin layers were partially etched by ionized N_2 gas exposure and transformed into roughened surfaces, i.e., ns-SiO_2. The chemical reaction should be as follows:

$$SiO_2(\text{layer})+N_2^+\rightarrow ns\text{-}SiO_2+NO\uparrow. \tag{1}$$

At $30\leqslant t_e\leqslant60$ min, the root-mean-square (rms) roughness decreases abruptly due to both etching and adsorption processes. However, for the sample of $t_e\geqslant60$ min, the rms roughness is diminished as the t_e increases. On the basis of XPS analysis, it can be confirmed that the adsorption of ionized nitrogen results in the ns-SiO_2 surface being covered with Si_3N_4 and SiO_xN_y compounds through the following chemical reactions:

$$Si+N_2^+\rightarrow Si_3N_4+Si, \tag{2}$$

$$ns\text{-}SiO_2+N_2^+\rightarrow ns\text{-}SiO_xN_y+ns\text{-}SiN_y. \tag{3}$$

In particular, the chemical reaction (2) is normally observed on the clean Si surface under ionized nitrogen exposure, resulting in the preferable formation of Si_3N_4 islands. In Fig. 2(e), the average rms of the morphology is summarized as a function of the exposing time t_e. In the range of the dominant etching process (i.e., $0\leqslant t_e\leqslant40$ min), the maximum roughness of ns-SiO_2 is approximately 3.7 nm corresponding to the thickness of the native SiO_2 layer on a Si substrate. The adsorption process is not initiated until the clean Si surface begins to appear due to the removal of the SiO_2 layer from Si at around $t_e=40$ min. Following this, the abrupt chemical reaction to form nitride compounds such as SiN_y, SiO_xN_y, and Si_3N_4 occurs with increasing t_e. Thus, it is proposed that the physicochemically modified structures are

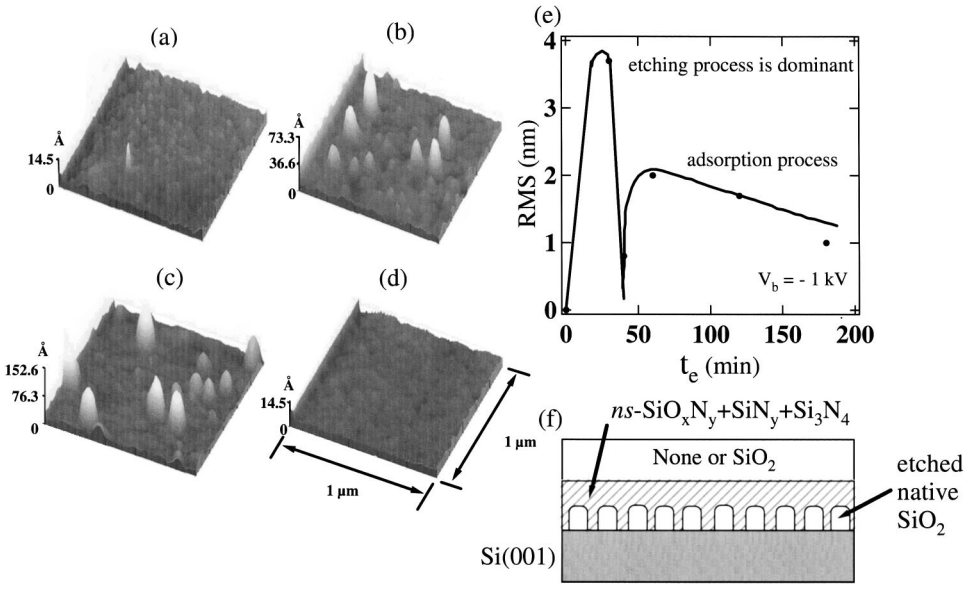

FIG. 2. The AFM images of SiO_2/Si samples with various exposure times (a) $t_e=30$, (b) 60, (c) 120, and (d) 180 min. (e) The average rms roughness of the surface as a function t_e. (f) Schematic diagram of the nanostructure formed.

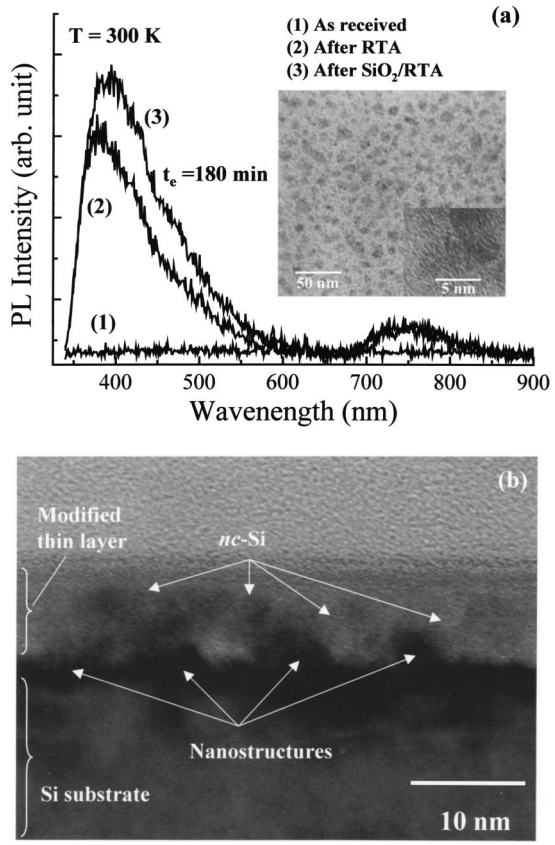

FIG. 3. (a) RT-PL spectra taken from ns-SiO_xN_y/ns-SiO_2/Si samples before and after RTA. The inset represents a HR-TEM image of the formed nc-Si structure. The average size of nc-Si was 6 nm and the average areal density was 4.6×10^{12} cm^{-2}. The enlargement of a local nc-Si region is also provided on the bottom right-hand side. (b) The cross-sectional HR-TEM image.

mainly composed of ns-SiO_xN_y/ns-SiO_2/Si as illustrated in Fig. 2(f). It should also be noted in this process that the SiO_xN_y and SiN_y compounds are formed at a nanometer scale, due to the formation of ns-SiO_2 at the initial stage of the chemical etching reactions. Thus, it is suggested that the ionized N_2 gas exposure is a simple, reproducible, and low-temperature process for fabricating the ns-SiO_xN_y/ns-SiO_2/Si structures, which differ from the common methods, such as chemical vapor deposition or sputtering techniques, that have been used for the formation of those structures.

A sample of $t_e=180$ min was adopted for the PL measurements. Figure 3(a) shows the PL spectra taken from the as-prepared sample and the rapid thermal annealed samples in an UHV chamber at 1000 °C for 1 min. In addition, 2–3 nm thick SiO_2 cap layers on top of the ns-SiO_xN_y/ns-SiO_2/Si structure were prepared and annealed under the same conditions, for comparative purposes. As shown in Fig. 3(a), RT-PL peaking at a wavelength of around 400 nm was obtained in the annealed samples, whereas no emission peak was observed in the as-prepared sample. Although the luminescent intensity is not as strong due to the single layer structure, the emission peak is clearly seen after the rapid thermal annealing (RTA) processes. Moreover, the higher PL intensity is observed for the SiO_2-capped sample. Better confinement of carriers is expected to enhance the PL efficiency for the SiO_2-capped sample. This reflects the fact that the PL spectra are related to the creation of nc-Si from the ns-SiO_xN_y/ns-SiO_2/Si structures through the RTA processes. No other chemical bonding states related to the PL spectra can be reasonably ruled out because all of the processes were performed *in situ* in the UHV chamber. Therefore, the RTA process performed in the UHV chamber results in the formation of nc-Si from the physicochemically modified ns-SiO_xNy/ns-SiO_2/Si structures, affecting the appearance of PL spectra.

In order to confirm the formation of nc-Si, a HR-TEM image of the plane view of the annealed sample was taken, as shown in the inset in Fig. 3(a). As expected from the AFM and PL measurements, the distribution of nc-Si was observed for all areas on the sample. The areal density of nc-Si is 4.6×10^{12} cm^{-2} with an average size of 6 nm. Figure 3(a) also shows an enlarged view of a local nc-Si region. The cross-sectional HR-TEM is provided in Fig. 3(b), indicating that the nearly single layer structure of nc-Si was formed in between nanostructures such as SiO_xN_y and SiO_2. The typical height of nanostructures were found to be less than approximately 5 nm which is in good agreement with the results of AFM measurement. It can be confirmed from the HR-TEM measurement that the nanostructures played a role of barrier against the random formation of nc-Si during the RTA processes.

In summary, the structure of nc-Si has been fabricated from *in situ* etching and adsorption processes on SiO_2/Si, using ionized nitrogen gas exposure at RT. The chemical reactions on the surface were monitored and analyzed quantitatively *in situ* by XPS. Both the etching process for ns-SiO_2/Si and the adsorption for ns-SiO_xN_y/ns-SiO_2/Si followed by *in situ* RTA, were the main procedures for the formation of a single layer structure of nc-Si. A typical nc-Si size of 6 nm and an areal density of 4.6×10^{12} cm^{-2} were obtained in a thin layer (10 nm in thickness), resulting in a PL peak of around 400 nm. It is, therefore, suggested that the present method can be applied to nanostructure formation using a low-energy and low-temperature process suitable for nanodevice applications.

This work was supported by Ministry of Information and Communication through ETRI under Contract No. 2M12090.

[1] J. Robertson, Nature (London) **418**, 30 (2002).
[2] S. Sriraman, S. Agarwal, E. S. Aydil, and D. Maroudas, Nature (London) **418**, 62 (2002).
[3] W. L. Ng, M. A. Lourenco, R. M. Gwilliam, S. Ledain, G. Shao, and K. P. Homewood, Nature (London) **410**, 192 (2001).
[4] L. T. Canham, Appl. Phys. Lett. **57**, 1046 (1990).
[5] J. P. Wilcoxon and G. A. Samara, Appl. Phys. Lett. **74**, 3164 (1999).
[6] G. M. Credo, M. D. Mason, and S. K. Buratto, Appl. Phys. Lett. **74**, 1978 (1999).
[7] S. Fujita and N. Sugiyama, Appl. Phys. Lett. **74**, 308 (1999).
[8] M. L. Brongersma, A. Polman, K. S. Min, E. Boer, T. Tambo, and H. A. Atwater, Appl. Phys. Lett. **72**, 2577 (1998).
[9] N.-M. Park, T.-S. Kim, and S.-J. Park, Appl. Phys. Lett. **78**, 2575 (2001).
[10] S. Cheylen, R. G. Elliman, K. Gaff, and A. Durandet, Appl. Phys. Lett. **78**, 1670 (2001).
[11] I. Vasiliev, S. Öğ üt, and J. R. Chelikowsky, Phys. Rev. Lett. **86**, 1813 (2001).
[12] S. Cheylan and R. G. Elliman, Appl. Phys. Lett. **78**, 1225 (2001).
[13] G.-M. Riganese, A. Pasquarello, J.-C. Charlier, X. Gonze, and R. Car, Phys. Rev. Lett. **79**, 5174 (1997).